Focusing quantum states on surfaces: A route towards the design of ultrasmall electronic devices

M. Sentef, A. P. Kampf, S. Hembacher, and J. Mannhart
Institute of Physics, Center for Electronic Correlations and Magnetism, University of Augsburg, 86135 Augsburg, Germany
(Received 7 September 2006; published 13 October 2006)

Does the size of atoms present a lower limit to the size of electronic structures that can be fabricated in solids? This limit can be overcome by using devices that exploit quantum mechanical scattering of electron waves at atoms arranged in focusing geometries on selected surfaces. Calculations reveal that features smaller than a hydrogen atom can be obtained. These structures are potentially useful for device applications and offer a route to the fabrication of ultrafine and well-defined tips for scanning tunneling microscopy.

DOI: 10.1103/PhysRevB.74.153407 PACS number(s): 85.35.−p, 73.20.−r, 73.63.−b

The manufacture of ever smaller objects is an ongoing pursuit of science and technology, which at the end of the 20th century led to the fabrication of nanometer-sized structures. A seminal highlight was accomplished in 1993 with the manipulation of single atoms,[1] which were even assembled into crystallites.[2] It obviously seems prohibited to construct even smaller structures. How could this be done?

Here, we explore the possibility to design ultrasmall electronic structures by manipulating electronic surface states of metals. We will present examples revealing that electron density peaks as small as 1 Å can be achieved. The width of the electronic peak is hereby limited only on the scale of the shortest wavelength of the surface band states. By shrinking the size of interference peaks of electronic surface states, new options for device application arise. Electron density peaks of Å width may, for example, be exploited as ultrafine and well-defined quantum states, to be used as tips in scanning tunneling microscopy (STM).

The approach discussed below builds on experimental investigations of electronic surface states. Electrons in Shockley surface states of metals can be scattered by surface steps and by individual atoms placed on the surface.[1,3,4] Complex interference patterns have been generated in artificially manufactured corrals of circular or elliptical shape.[5,6] Even quantum mirage phenomena have been induced in such corrals.[7–9] In quantum corrals, electrons are focused on well-defined areas on the surface, thereby creating locations with an enhanced local density of states and therefore an enhanced electron density with typical sizes of 1–2 nm. This work has opened a route for manipulating quantum states almost on the atomic level and raises the question whether it is possible to design arrangements of atoms with optimized focusing properties for quantum waves. Can quantum structures on sub-Å length scales be realized?

Fundamental as well as practical problems are encountered on the road to sharply focused quantum states. First, one may ask whether Heisenberg's uncertainty principle[11] ultimately sets a limit for the spatial extent of fine structure in a quantum mechanical wave function. On the practical side, the rules of optics cannot be applied to design the focusing structures for quantum waves. This is because electronic waves with short wavelengths are needed to finely focus the electrons, but scattering of such high-energy particles involves anisotropic non-*s*-wave channels. Since the higher angular momentum scattering channels have no counterpart in classical wave mechanics, the design rules of conventional optical instruments cannot be used to device instruments for focusing quantum mechanical waves with short wavelengths.

Using model calculations of surface wave scattering from hard spheres, we consider here focusing arrangements built from scattering centers (see Fig. 1), designed to achieve ultranarrow peak widths. Complex interference patterns are obtained and analyzed for parabolic and semielliptic geometries. It is shown that in this way locally enhanced electron densities with sub-Å lateral size can be realized.

The guiding idea for our approach is to design quantum mechanical (electronic) states $\Psi(\mathbf{r},\mathbf{p})$ with effective widths Δr and Δp in real space and in momentum space, respectively, such that $|\Psi|^2$ forms a spike of width Δr^*. Heisenberg's uncertainty relation requires that $\Delta r \Delta p \geqslant \hbar/2$, where $\hbar$ is Planck's constant. While this fundamental principle of quantum mechanics inevitably controls any measurement process, it is important that the uncertainty relation does not preclude the possibility to structure the electronic wave function on a length scale Δr^* much smaller than Δr. Therefore, the principles of quantum mechanics do not set a lower limit for generating ultrasmall electronic structures, although these will possibly have a small local probability density in the spike volume. Rather, in a superposition of quantum mechanical waves, Δr^* is often limited by the largest available momentum, which thereby imposes an upper limit on Δp. For the purpose of focusing electronic waves in a crystalline solid this suggests to use high-energy waves preferentially in band states with a large effective mass.

To explore the size of the smallest area into which the electrons can be focused with practical experimental setups, we performed model calculations in two space dimensions. Scattering centers of radius r_0 are arranged in open focusing geometries with either parabolic or semielliptic shape (see Fig. 1). An electronic surface wave, generated, for example, by a tunnel junction, is considered to enter the focusing arrangement as a plane wave with wave vector $\mathbf{k}$. The wave propagates along the symmetry axis of a regular arrangement of hard disks, with which we model individual atoms placed on a metallic surface with a spacing $d \sim 10 r_0$ as is typical for Fe adatom corrals.[1,5] For long wavelengths $\lambda \gg r_0$, realized for surface state electrons on copper (111) surfaces, only isotropic *s*-wave scattering is significant. In this case, multiple scattering events and absorption from the scattering

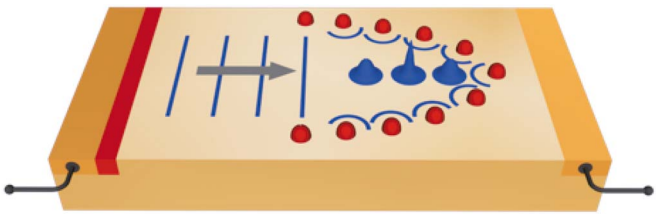

FIG. 1. (Color online) Schematic view of the focusing geometry. An electronic surface wave is generated with a tunnel junction and propagates towards an arrangement of scattering centers (red semispheres). Multiple interference peaks emerge from the superposition of scattered waves.

centers can be straightforwardly considered.[5] For shorter wavelengths, the established scattering analysis must be extended to include higher angular momentum scattering channels.

In the absence of multiple scattering the scattering state has the asymptotic form (for $kr \gg 1$)

$$\psi(\mathbf{r}) \simeq e^{i\mathbf{k}\cdot\mathbf{r}} + \sum_{\nu} f(\vartheta_\nu) e^{i\mathbf{k}\cdot\mathbf{R}_\nu} \frac{e^{ikr_\nu}}{\sqrt{kr_\nu}}, \tag{1}$$

where $\mathbf{R}_\nu$ denotes the position of the νth scattering center, and $\mathbf{r}_\nu = \mathbf{r} - \mathbf{R}_\nu$ with polar coordinates r_ν and ϑ_ν measures the relative position to the disk at $\mathbf{R}_\nu$. Introducing partial wave phase shifts, the scattering amplitude follows as

$$f(\vartheta) = \sqrt{\frac{2i}{\pi}} \left(e^{i\delta_0} \sin\delta_0 + \sum_{m=1}^{\infty} 2e^{i\delta_m} \sin\delta_m \cos m\vartheta \right). \tag{2}$$

The parameter m counts the scattering channel; the corresponding phase shifts are determined by $\tan\delta_m = J_m(kr_0)/N_m(kr_0)$, where J_m and N_m denote the Bessel functions of the first and second kind, respectively.

In the restriction to s-wave scattering, repeated scattering events are included by extending Eq. (1) to[5]

$$\begin{aligned} \psi(\mathbf{r}) &\simeq e^{i\mathbf{k}\cdot\mathbf{r}} + \mathbf{b}_T \cdot (\mathbf{1} + \mathbf{A} + \mathbf{A}^2 + \mathbf{A}^3 + \cdots) \cdot \mathbf{a}(\mathbf{r}) \\ &= e^{i\mathbf{k}\cdot\mathbf{r}} + \mathbf{b}_T \cdot (\mathbf{1} - \mathbf{A})^{-1} \cdot \mathbf{a}(\mathbf{r}). \end{aligned} \tag{3}$$

Here, $\mathbf{b} = (b_1, \ldots, b_N)$ for N scattering centers with $b_\nu = e^{i\mathbf{k}\cdot\mathbf{R}_\nu}$ accounts for the phase factors related to the individual disk positions. The amplitudes for the waves scattered from the disk at $\mathbf{R}_\nu$ to the disk at $\mathbf{R}_\mu$ $(\nu \neq \mu)$ form an $N \times N$ matrix with

$$A_{\nu\mu} = f_0 \frac{e^{ikr_{\nu\mu}}}{\sqrt{kr_{\nu\mu}}}, \tag{4}$$

where $r_{\nu\mu} = |\mathbf{R}_\nu - \mathbf{R}_\mu|$. Similarly, the amplitude of the wave scattered from $\mathbf{R}_\mu$ to $\mathbf{r}$ is

$$a_\mu(\mathbf{r}) = f_0 \frac{e^{ikr_\mu}}{\sqrt{kr_\mu}}. \tag{5}$$

The scattering amplitude f_0 is related to the s-wave phase shift δ_0 by

$$f_0 = \sqrt{\frac{2i}{\pi}} e^{i\delta_0} \sin\delta_0 = \frac{1}{\sqrt{2\pi i}} (e^{2i\delta_0} - 1). \tag{6}$$

The possible partial absorption of the incident electronic surface wave by inelastic scattering and scattering into bulk states is incorporated by allowing the phase shifts to become complex,[5] corresponding to the replacement $e^{2i\delta_0} \to \alpha_0 e^{2i\delta_0}$ in Eq. (6). Henceforth, δ_0 is a real number; the absorption coefficient α_0 is 1 for nonabsorbing adatoms and vanishes for complete attenuation.

For wavelengths which become almost comparable to the size of an atom, higher angular momentum scattering channels are important. To give an example, for $kr_0 = 2\pi r_0/\lambda = 1.24$ (see below) the scattering phase shifts in s, p, and d channels are $\delta_0 = 69°$, $\delta_1 = -41°$, and $\delta_2 = -8°$. With the restriction to double scattering from each disk the ansatz for the asymptotic scattering state is extended to

$$\begin{aligned} \psi(\mathbf{r}) \simeq e^{i\mathbf{k}\cdot\mathbf{r}} &+ \sum_{\nu=1}^{N} e^{i\mathbf{k}\cdot\mathbf{R}_\nu} f(\vartheta_\nu) \frac{e^{ikr_\nu}}{\sqrt{kr_\nu}} \\ &+ \sum_{\mu,\nu=1;\mu\neq\nu}^{N} e^{i\mathbf{k}\cdot\mathbf{R}_\nu} f(\vartheta_{\nu\mu}) \frac{e^{ikr_{\nu\mu}}}{\sqrt{kr_{\nu\mu}}} f(\vartheta_\mu - \vartheta_{\nu\mu}) \frac{e^{ikr_\mu}}{\sqrt{kr_\mu}}, \end{aligned} \tag{7}$$

where $\vartheta_{\nu\mu}$ is the angle for the position of the scattering disk μ in the polar coordinate system attached to disk ν. Without absorption, and neglecting the still small contribution of the d-wave scattering channel, only the s- and p-wave contributions ($m=0$ and $m=1$) are included in the angular dependent scattering amplitude given in Eq. (2).

In a first attempt, the focusing properties of a device consisting of two parabolic "quantum mirrors" arranged like a reflector telescope have been calculated. The substrate was assumed to be the Cu (111) surface, and 29 hard disks with radius $r_0 = 0.63$ Å were chosen to present Co^{3+} ions as scatterers. The focal distance of the parabola is $f = 4.9$ Å, and the average disk spacing is 8 Å. The wavelength of the incoming wave was taken to be $\lambda = 12$ Å. At this wavelength $\lambda \gg r_0$, so that only s-wave scattering must be considered. In Fig. 2 we show the resulting absolute square $|\psi(\mathbf{r})|^2$ of the scattering state. Guided by the successful quantitative analysis of the current-voltage characteristics at the center of a circular quantum corral of iron atoms on a copper surface,[5] the "black dot" attenuation limit $\alpha_0 = 0$ was adopted. The image shown in Fig. 2 is the pattern that would be observed in a standard STM local density of states measurement.

Near the tip of the parabola intense interference peaks with a full width at half maximum (FWHM) ~4.2 Å are produced (see, for example, peak A in Fig. 2). Due to the

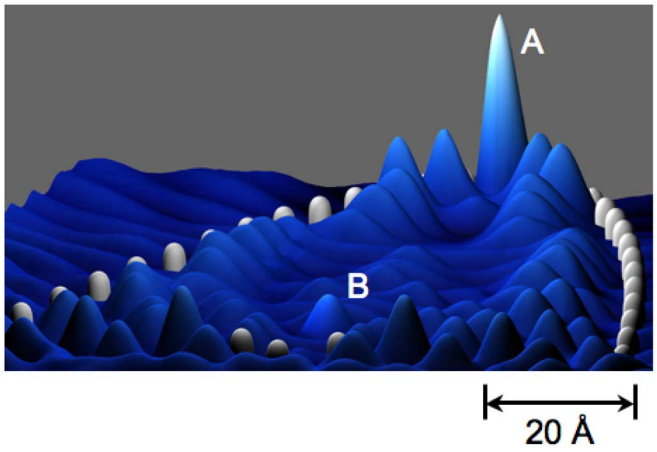

FIG. 2. (Color online) Focusing of an electron wave with wavelength 12 Å by scattering from two quantum mirrors. The arrangement consists of a large parabolic mirror formed by 29 scattering centers (white pillars) and a small mirror consisting of three additional scatterers in a reflector telescope geometry. The plot shows the distribution $|\psi(\mathbf{r})|^2$ of the electronic scattering state. Only *s*-wave scattering is included. "*A*" marks the most prominent peak near the tip, while the peak "*B*" emerges near the focus point as a result of the quantum mirror geometry.

$1/\sqrt{r}$ decay of the amplitude for the scattered waves the peak heights are larger the closer the peaks are to the scattering atom.[13] Resulting from the focusing of the second, smaller "quantum mirror" additional peaks emerge near its focal point (see, for example, peak *B* in Fig. 2). The width of peak *B*, ~3.5 Å at FWHM, is just fractions of the incoming wavelength. The peak, however, has a small intensity.

There are obvious routes to further improve the focusing. First, materials capable of sustaining surface waves with considerably smaller wavelengths may be used. The goal to achieve interference peaks with subatomic widths precludes the use of surface eigenstates of noble metal surfaces, whose typical wavelengths are ~15 Å.[12] The recently observed Friedel oscillations on beryllium (0001) surfaces with wavelengths as short as 3.2 Å (Ref. 10) suggest Be as a candidate material. Other options for tuning the electronic density distribution include using nonmonochromatic waves and optimizing the arrangement of the surface adatom scatterers and the geometry of the quantum mirror. The development of a mathematical algorithm to select a focusing arrangement is quite a nontrivial task, and we have therefore explicitly tried several device geometries. Of the ones explored, particularly sharp peaks were obtained by using a semiellipse, as we will demonstrate in the following.

As shown in Fig. 3, 17 hard disks were placed on the contourline of a semiellipse with eccentricity $e=0.5$ and an average disk spacing of 6 Å. In this calculation the wavelength of the incoming wave of 3.2 Å and a disk radius of again $r_0=0.63$ Å was chosen. Figure 3 shows the resulting contour plot of $|\psi(\mathbf{r})|^2$ for the scattering state calculated from Eq. (7). The complex structures in this interference pattern originate in part from the angular dependent *p*-wave scattering channels; the *p*-wave channels have no counterpart in classical geometrical optics. Figure 4 shows a larger magnification of the area marked by the white dashed square in Fig. 3. This area contains the most prominent constructive interference peak in this semielliptic focusing quantum mirror geometry. The peak has an anisotropic shape with an almost elliptic cross section; along the horizontal direction the FWHM of this peak is merely 0.92 Å. This is less than 2 Bohr radii. The peak width is therefore smaller than the nominal size of the 1 s orbital of hydrogen.

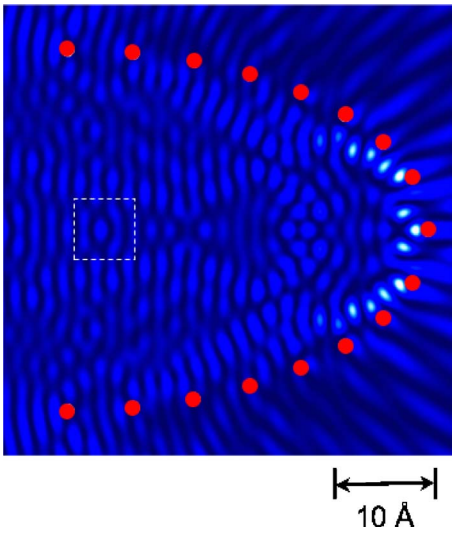

FIG. 3. (Color online) Distribution of an electron scattering state $|\psi(\mathbf{r})|^2$ achieved by scattering from a semielliptic arrangement. The wavelength of the incoming wave is $\lambda=3.2$ Å—the wavelength of Friedel oscillations on Be (0001) surfaces. *s*- and *p*-wave scattering channels are included.

So far we have not made an attempt to uniquely determine the optimum disk arrangement, which leads to the sharpest interference structure. Alternative focusing geometries with different selected positions of the scattering centers may very well lead to even sharper interference peaks. Initial ideas of "wave function engineering" by a special-purpose design of quantum corral geometries have recently been formulated in

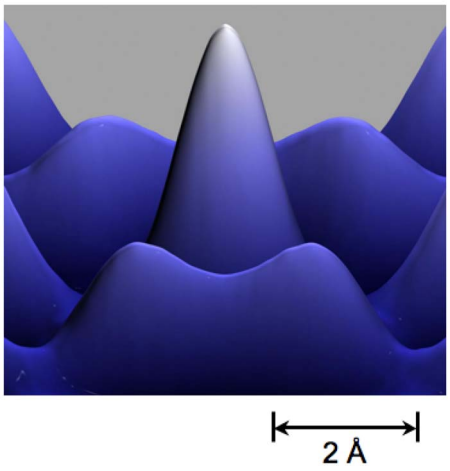

FIG. 4. (Color online) Magnification of the area marked by the white, dashed square in Fig. 3. The width of this peak of the electron density is 0.92 Å (FWHM).

the attempt to generate special predefined mirage phenomena.[14] It is likely that similar strategies can be followed to identify arrangements of scattering centers with optimized focusing properties. If surface waves with wavelengths of just a few Å are considered, such optimization strategies will necessarily have to include also non-*s*-wave scattering channels.

Our calculations reveal in a proof-of-principle that special arrangements of individual atoms on surfaces allow to create electron states with diameters comparable to the size of a hydrogen atom. These states may be coupled to bulk states and be used in devices such as highly focused sources of tunneling electrons, as, for example, required for STM tips. The focusing of spin polarized surface states may furthermore allow to image magnetic structures on the atomic or subatomic scale. The controlled design and device applications of electronic structures on the sub-Å scale may therefore emerge as a real possibility.

The authors thank F. Giessibl, D. Vollhardt, G. Schön, Ø. Fischer, M. Sekania, C. W. Schneider, T. Kopp, R. Claessen, and D. Pohl for thoughtful discussions. This work was supported by the BMBF (EKM-project 13N6918) and the Deutsche Forschungsgemeinschaft (SFB 484).

[1] M. F. Crommie, C. P. Lutz, and D. M. Eigler, Nature (London) **363**, 524 (1993); Science **262**, 218 (1993).

[2] See the IBM homepage at http://www.almaden.ibm.com/vis/stm/hexagone.html

[3] Y. Hasegawa and P. Avouris, Phys. Rev. Lett. **71**, 1071 (1993).

[4] L. Bürgi, O. Jeandupeux, H. Brune, and K. Kern, Phys. Rev. Lett. **82**, 4516 (1999).

[5] E. J. Heller, M. F. Crommie, C. P. Lutz, and D. M. Eigler, Nature (London) **369**, 464 (1994).

[6] J. Kliewer, R. Berndt, E. V. Chulkov, V. M. Silkin, P. M. Echenique, and S. Crampin, Science **288**, 1899 (2000).

[7] H. C. Manoharan, C. P. Lutz, and D. M. Eigler, Nature (London) **403**, 512 (2000).

[8] The theoretical work on quantum corrals and mirages was recently reviewed by G. A. Fiete and E. J. Heller, Rev. Mod. Phys. **75**, 933 (2003).

[9] See also A. A. Aligia and A. M. Lobos, J. Phys.: Condens. Matter **17**, S1095 (2005) and references therein.

[10] P. T. Sprunger, L. Petersen, E. W. Plummer, E. Lægsgaard, and F. Besenbacher, Surf. Sci. **275**, 1765 (1997).

[11] W. Heisenberg, Z. Phys. **43**, 172 (1927).

[12] S. G. Davison and M. Steslicka, *Basic Theory of Surface States* (Oxford, New York, 1996).

[13] Because we use the asymptotic form for the scattered waves, which is only very accurate on distances larger than 5 atomic radii, the amplitude for $\psi(\mathbf{r})$ is overestimated in the very near vicinity of each scattering disk.

[14] A. A. Correa, F. A. Reboredo, and C. A. Balseiro, Phys. Rev. B **71**, 035418 (2005).